

Neutron Diffraction Study of the Structures and Magnetic Properties of Manganese Bismuthide*

B. W. ROBERTS

General Electric Research Laboratory, Schenectady, New York

(Received July 5, 1956)

The intermetallic compound, BiMn, has been studied by neutron diffraction at temperatures from 4.2°K to 733°K (460°C). In the temperature range 340–360°C a disordered arrangement of Mn atoms on regular and interstitial lattice sites fits the data well if the Mn atoms are assumed to be in the paramagnetic state. This model conflicts with the suggestion made by Guillaud of an antiferromagnetic state in this temperature range. The temperature hysteresis associated with both magnetization and the large cell distortions are qualitatively explained by the disordering and recovery at the transformation temperatures. The effective moment per Mn atom below the transformation agrees with the magnetic measurements of Heikes within experimental error. Measurements of spin direction made at temperatures below 84°K show that only partial rotation occurs in zero magnetic field.

INTRODUCTION

THE stoichiometric alloy, BiMn, has been found to have several unusual magnetic properties. The extensive study of Guillaud¹ has shown that BiMn is ferromagnetic from very low temperature to 360°C with increasing temperature and upon cooling exhibits a hysteresis in the magnetization with recovery occurring at about 340°C. The loss and recovery of magnetization is discontinuous. Upon the evidence of the hysteresis and discontinuous drop in magnetization plus magnetic susceptibility measurements, which yielded a maximum at 445°C, Guillaud² proposed an antiferromagnetic state between 340–360°C, and 445°C and a paramagnetic state above this temperature. At room temperature BiMn was found by Guillaud to have the highest known magnetocrystalline energy, 11.2×10^6 ergs/cc. This was confirmed by Williams, Sherwood, and Boothby³ who found a value for K_1 of 9.1×10^6 ergs/cc. The magnetocrystalline energy was found to decrease rapidly with decreasing temperature and to pass through zero at 84°K suggesting a rotation of the magnetic moments from along the c_0 axis of the NiAs type hexagonal crystal structure to positions in the basal plane. The ferromagnetic arrangement is shown in Fig. 1.

Guillaud⁴ also obtained x-ray evidence for changes in cell edge dimensions of BiMn quenched from above and below the 340–360°C transformation temperatures to room temperature. Willis and Rooksby⁵ obtained the cell edges at temperature and found nearly a 3% contraction of the c_0 axis upon heating near the point where the magnetization drops discontinuously to zero. No apparent change in crystal symmetry occurred.

* Neutron diffraction experiments were carried out at the Brookhaven National Laboratory Reactor, Upton, New York.

¹ C. Guillaud, thesis, University of Strasbourg, 1943 (unpublished).

² C. Guillaud, *J. phys. radium* **12**, 143 (1951).

³ Williams, Sherwood, and Boothby, *Bull. Am. Phys. Soc. Ser. II*, **1**, 132 (1956).

⁴ C. Guillaud, *J. phys. radium* **12**, 223 (1951).

⁵ B. T. M. Willis and H. P. Rooksby, *Proc. Phys. Soc. (London)* **B67**, 290 (1954).

The magnetic moment per manganese atom of BiMn has been reported with a variety of moments due probably to the difficulty in preparation of a pure alloy. Thielmann⁶ found $3.13\mu_B$; Galperin,⁷ $2.74\mu_B$; Guillaud,¹ $3.52\mu_B$; and recently Heikes⁸ has found an extrapolated value of $3.9\mu_B$ for the moment at saturation. No discontinuity in the magnetization curve¹ was associated with the apparent change in easy direction of magnetization at 84°K.

Heikes⁸ has found BiMn quenched from above the transformation temperature to be ferromagnetic at room temperature with an approximate saturation moment of $1.7\mu_B$ per Mn atom and a Curie temperature near 200°C. Upon heating above 200°C, the saturation moment recovered to the equilibrium state value. Guillaud,² in contrast, observed no moment on samples

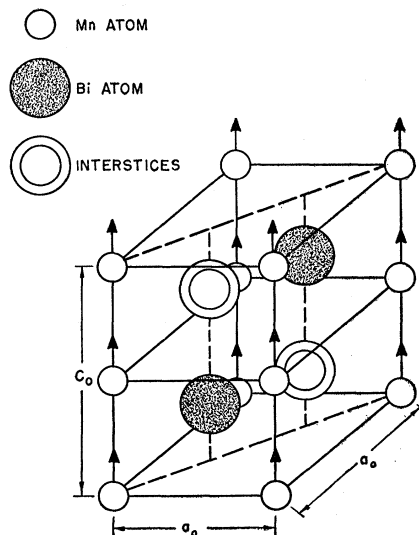


FIG. 1. Structure of BiMn with interstitial positions indicated (NiAs type). Moments indicated along c_0 .

⁶ K. Thielmann, *Ann. Physik* **37**, 41 (1940).

⁷ F. Galperin, *Doklady Akad. Nauk U.S.S.R.* **75**, 647 (1950).

⁸ R. R. Heikes, *Phys. Rev.* **99**, 446 (1955).

quenched from above 340–360°C, but found recovery to occur near 200°C. The extrapolation of reciprocal susceptibility⁸ to ~170°C supports this observation of a metastable ferromagnetic phase with the paramagnetic state existing in the range where antiferromagnetism was suggested by Guillaud. Susceptibility measurements by McGuire and Varela⁹ on less pure BiMn alloy also suggest the paramagnetic state in this region. Upon heating above 200°C, the high-temperature BiMn phase recovered to the stable phase with the equilibrium saturation magnetization value of 3.9₆μ_B. Adam and Standley¹⁰ have estimated a *g* value at –180°C of 2.4 for BiMn.

A combination of the very large magnetocrystalline energy plus a fine particle size has yielded material with both high coercive force and large energy product.^{11,12} BiMn has been assigned a very large magnetostriction constant³ of 800×10^{–6} at saturation.

In view of the conflict of evidence for the antiferromagnetic state above the magnetic transition temperature, the evidence for the rotation of moments at 84°K, the discontinuous loss in magnetization, and the remaining unusual properties of BiMn, the following neutron diffraction experiments were carried out.

EXPERIMENTAL

Neutron diffraction data were obtained with a lead-crystal-monochromatized neutron beam and a high-resolution spectrometer similar to that described by Corliss and Hastings.¹³ For low-temperature observations a two-stage cryostat similar to that of Erickson¹⁴ was used to obtain temperatures down to 4.2°K.

SAMPLE PREPARATION

Preparation of high-purity BiMn alloy is difficult, first because of decomposition above 445°C to molten

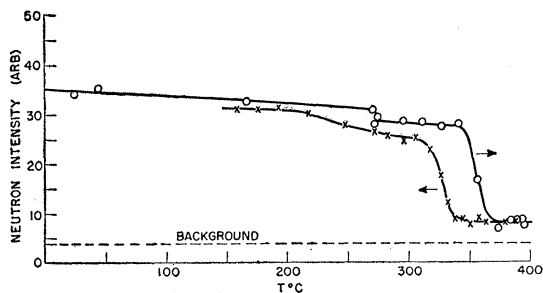


Fig. 2. Hysteresis demonstrated by (100) peak intensity.

⁹ T. McGuire and J. O. Varela, Naval Ordnance Laboratory, Silver Spring, Maryland (unpublished work). Also, see A. J. P. Meyer and P. Taglang, *J. phys. radium* **12**, 63S (1951).

¹⁰ G. D. Adam and K. J. Standley, *Proc. Phys. Soc. (London)* **A66**, 823 (1953).

¹¹ Adams, Hubbard, and Syeles, *J. Appl. Phys.* **23**, 1207 (1952).

¹² E. V. Shtolts and Ya. S. Shur, *Doklady Akad. Nauk U.S.S.R.* **95**, 781 (1954).

¹³ Corliss, Hastings, and Brockman, *Phys. Rev.* **90**, 1013 (1953).

¹⁴ R. A. Erickson, *Phys. Rev.* **90**, 779 (1953).

bismuth and α-Mn and secondly because below 445°C complete reaction of Bi and Mn to form BiMn is hampered by the greatly reduced diffusion through the BiMn after formation. A recent phase diagram study by Seybolt *et al.*¹⁵ discusses these difficulties. The BiMn sample used principally in this study, hereafter denoted "NOL" was kindly supplied by Mr. Edmund Adams of the Naval Ordnance Laboratory. The BiMn was hot-pressed¹¹ into cylinders of approximately 2-cm diameter and 1.5-cm length in zero magnetic field to avoid magnetic orientation effects. An intrinsic coercive force of 2400 oersteds was measured on a sample pressed from the same powder, which suggests an effective average particle size of 28 microns. Chemical analysis made after all experiments were carried out yielded the weight percent composition in Table I. An independent composition check made by comparing the initial neutron intensities observed at room temperature is also shown. A small increase in MnO content is noted. No evidence for preferred orientation of the sample was found when neutron intensities from the cylinders stacked as a flat sample were compared to intensities observed from the vertical cylinder array. The MnO present appeared to be distributed throughout the cylinders. The presence of free Bi and MnO with the BiMn must be considered in the following observations.

DEMONSTRATION OF MAGNETIC HYSTERESIS

A highly oriented bar of BiMn alloy with excess Mn and Bi was prepared by heating pressed powders at 320°C for 25 hours while held in a magnetic field of approximately 9000 oe. The average BiMn grain size was 200 microns. The resulting field-oriented BiMn sample was mounted on the neutron spectrometer with *c*₀ axis vertical and the (100) reflection maximized. Growth in the magnetic field controlled only the orientation of the magnetic axis (*c*₀) so that the *a*₀ axes were directed at random in a plane perpendicular to *c*₀. The peak intensity was studied with the sample in air as a function of temperature as illustrated in Fig. 2. Upon passing through the melting point of Bi (271°C), a small discontinuity is observed which suggests a small dissolution of BiMn or some loss of crystallite orientation. As *T* increases, the (100) peak intensity drops

TABLE I. Composition by weight of BiMn (NOL) sample.

Neutron diffraction analysis ^a		Chemical analysis	
Bi	75.4%	Bi	73.5%
Mn	22.1	Mn	23.4
O	2.5	O	3.1 ^b

^a The neutron diffraction analysis gave BiMn—65.6%; Bi—23.5%; MnO—10.9%; Mn—nil.

^b Difference of % Bi+% Mn from 100% assumed to be oxygen. This is high.

¹⁵ Seybolt, Hansen, Roberts, and Yurcisin, *J. Metals* **8**, 606 (1956).

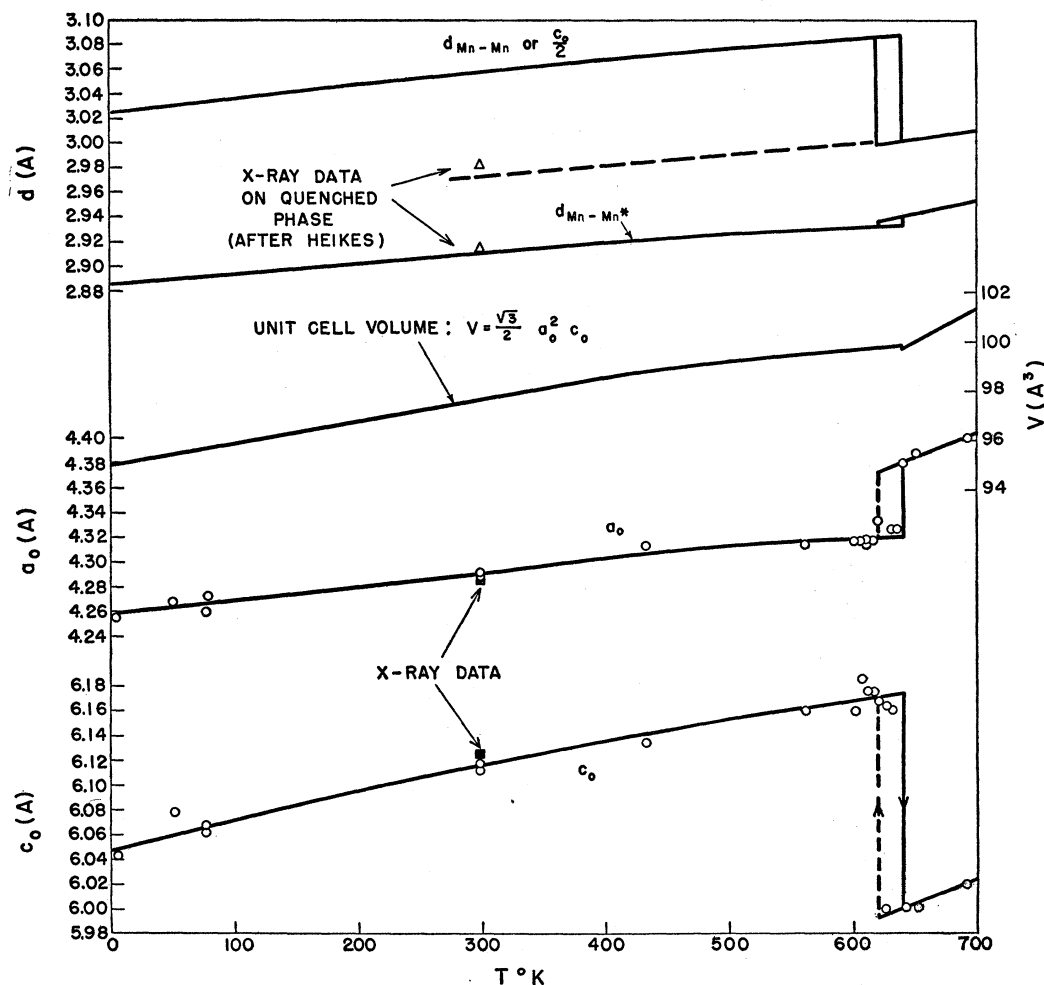


FIG. 3. BiMn cell edges, volume and Mn-Mn distances measured at temperature.

rapidly near 360°C , upon cooling recovers at 330°C and then slowly approaches the initial intensity after dissolution. The time intervals between points were about 3 min. Small scattering-angle adjustments were made to compensate for cell edge changes. The qualitative hysteresis shown here is broader than that found by Guillaud because of the large specimen mass.

CELL EDGES VS TEMPERATURE

Figure 3 shows the cell edges of hexagonal BiMn observed at temperature by neutron diffraction. X-ray data taken at room temperature are shown for comparison. The high-temperature portion of the curves agrees well with x-ray diffraction data of Willis and Rooksby.⁵ No significant volume change is observed at the transition temperature. The 340 and 360°C transformations were discontinuous within 5°C as found by Heikes⁸ and the c_0 axis contracts 3.0% upon loss of magnetization. This contraction is orders of magnitude greater than that observed at the Curie temperature for other ferromagnetic materials. The c/a ratio from

these data varies from 1.42_0 to 1.42_8 from liquid helium temperature to 360°C and above 340°C is close to 1.37 , showing a decrease of 4.2% at the transition.

ROOM TEMPERATURE MAGNETIC STRUCTURE

Figure 4(a) is a trace of the NOL BiMn sample taken at room temperature with the sample in rotation. Evidence for small amounts of crystalline Bi and MnO is present. Fortunately, a separation of these impurity diffraction effects could be clearly made. The intensities attributed to BiMn are shown in Table II as P_{obs} with data essential for calculation of relative intensities. No attempt to place the following observations on an absolute basis was made because of the presence of Bi and MnO. The predicted coherent nuclear and magnetic neutron scattering is given by:

$$P_{\text{calc}} = \frac{kjA(\mu r)}{\sin\theta \sin 2\theta} (F^2 + F_{\text{mag}}^2 p^2 q^2) \times \exp[-(C \cos^2 \varphi + 2B)(\sin^2 \theta)/\lambda^2], \quad (1)$$

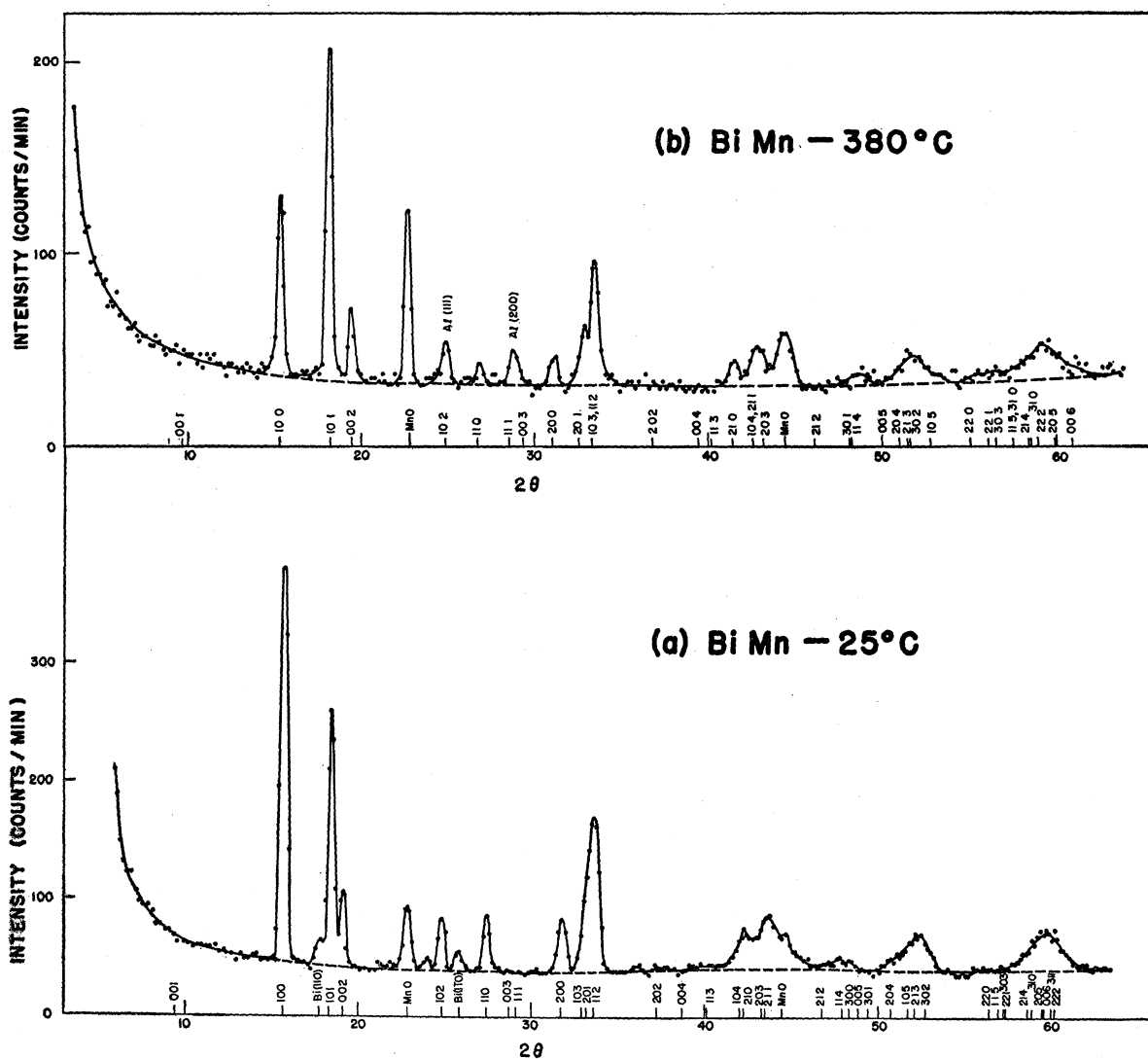


FIG. 4. Neutron diffraction traces of NOL BiMn. (a) Room temperature; (b) at 380°C.

where $k = \text{constant}$, $j = \text{multiplicity}$, $A(\mu r) = \text{cylindrical absorption correction}$, $\mu = \text{linear absorption coefficient}$, $r = \text{sample radius}$, $\theta = \text{Debye angle}$, $F = \text{crystal structure factor}$ $\sum_n b_n e^{2\pi i(hx+ky+lz)}$, $b_n = \text{scattering amplitude for neutrons}$ ($b_{\text{Mn}} = -0.368 \times 10^{-12}$ cm, $b_{\text{Bi}} = 0.850 \times 10^{-12}$ cm for this study), $F_{\text{mag}} = \text{magnetic structure factor}$, $q^2 = \sin^2(\mathbf{e} \cdot \mathbf{K})$, $\mathbf{e} = \text{unit scattering vector}$, $\mathbf{K} = \text{unit vector parallel to spin direction}$, $C = \text{empirical constant for directional temperature factor}$, $B = \text{conventional temperature factor}$, $\lambda = \text{neutron wavelength}$, $\varphi = \text{angle between } c_0 \text{ axis and crystal plane normal}$. The magnetic moment amplitude ϕ is given by

$$\phi = (e^2 \gamma / mc^2) f S = 0.538 f S \times 10^{-12} \text{ cm}, \quad (2)$$

where γ is the neutron magnetic moment, f is the magnetic form factor, and S is the electronic spin.

The observed intensities at 25°C may be interpreted

by picturing ferromagnetically aligned moments on each manganese atom of magnitude $3.8 \pm 0.3 \mu_B$ which are directed along the c_0 axis. The orbital moments are considered to be quenched. The crystal structure is of NiAs type. In Table II, the calculated magnetic intensities are listed under P_{calc}^M . The major magnetic intensity is in (100) with significant contributions from three lesser reflections. P_{calc} gives the combined nuclear and magnetic intensities and good intensity agreement is observed. The calculated and observed intensities are normalized at the (101) reflection which is solely nuclear in origin.

Use of the form factor of Shull¹⁶ for the state Mn^{++} yields for these data an apparent moment per manganese atom of $4.3 \mu_B$ at room temperature. This value is in conflict with existing room temperature moment data,

¹⁶ Shull, Strauser, and Wollan, Phys. Rev. **83**, 333 (1951).

the most reliable of which is that of Heikes,⁸ $3.6\mu_B$. To resolve this discrepancy we have chosen a form factor, Curve (b), Fig. 5, which yields a moment of $3.8\mu_B$ at room temperature for BiMn. Curve (a) is the form factor attributed to the Mn^{++} state and Curve (c) is the form factor found¹³ for $MgFe_2O_4$ and $NiFe_2O_4$. A fit of the BiMn neutron data could be made using the Heikes moment of $3.6\mu_B$, but the form factor would be unusual in shape being close to unity out to the first observed point. The experimental error limits on the Mn^{++} form factor would overlap but the mean positions at points of observations are always greater by more than 10%.

To demonstrate *qualitatively* the required shift of $3d$ electron density to effect the difference in form factors plotted in Fig. 5, the electron density distributions were calculated using^{16,17}

$$u(r) = \frac{2r}{\pi} \int_0^\infty x f_x \sin(rx) dx, \quad (3)$$

where $x = 4\pi(\sin\theta)/\lambda$, f_x is the form factor at x , and r is the radius in angstroms.

Figure 6 [Curve (a)] shows the $3d$ electron distribution of Mn^{++} as found by Shull, Strauser, and Wollan.¹⁶ Curve (b) is the distribution calculated in the same manner for the Mn in BiMn form factor except that $\mu(r)$ has been multiplied by 0.8 to approximately normalize the curves having assumed five $3d$

TABLE II. BiMn neutron data. 25°C.

<i>hkl</i>	P_{calc}^M	p^2/f^2	P_{calc}	P_{obs}
001	0		0	Nil*
100	570	0.885	987	987
101	0		520 ↔	520
002	0		209	177
102	99	0.49	100	99
110	85	0.34	136	125
003	0		0	Nil
111	0		0	Nil
200	39	...	145	166
103	0			
201	0			
112	34	...		
202	16	0.11	17	19
004	0		7	Nil
113	0		0	Nil
104	1	...		
210	5	...		
203	0			
211	0			
212	0		1	Nil
300, 114	...		45	54
005	...		0	Nil
301	...		0	Nil
(204, 105, 213, 302)	...		396	419
220	...		13	32
115, 303, 221	...		0	Nil
(214, 310, 205, 006, 311, 222)	...		474	484

$a_0 = 4.287\text{\AA}$, $c_0 = 6.126\text{\AA}$, $\lambda = 1.014\text{\AA}$, $C = 2.5\text{\AA}^2$,
 $2B = 0.5\text{\AA}^2$, $\mu r = 0.4$, $n = 3.8 \pm 0.3\mu_B$.

* "Nil" indicates no evidence for a reflection (< 10).

¹⁷ G. E. Bacon, *Neutron Diffraction* (Clarendon Press, Oxford, 1955), p. 142.

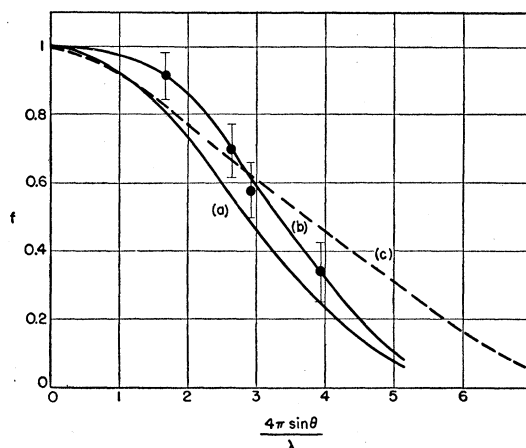


FIG. 5. Magnetic form factor curves of (a) Mn^{++} ; (b) BiMn; (c) $MgFe_2O_4$ and $NiFe_2O_4$.

electrons present for the Mn^{++} state and four for the state of Mn in BiMn. A slight shift to smaller radius of the $3d$ electron distribution is evident as would be suggested by the tighter binding of the $3d$ electrons in the assumed Mn^{+++} configuration. Because of the errors present, this comparison must be considered tentative.

MAGNETIZATION CURVE

The NOL BiMn cylindrical samples were hermetically sealed after flushing with He gas, into an aluminum container for high-temperature study. To obtain a magnetization curve, the (100) neutron intensity was studied as a function of temperature up to 420°C (693°K). A partial trace was made at 330°C (data given in Table III), just below the magnetic transformation which along with the complete trace at 25°C allowed a careful comparison of nuclear and magnetic contributions to the (100) reflection as a function of temperature. In Fig. 7 is plotted the resulting curve in comparison with that observed by Heikes.⁸ The magnetization curve determined by neutron diffraction parallels at high temperature that of Heikes measured directly by the gradient method. However, the neutron curve is roughly 10% greater at high temperature, slowly approaches Heikes' magnetization curve near 200°K, and finally dips below at very low temperature. The low-temperature observations will be discussed later.

Data were taken from the sample cooled into the hysteresis region as shown by the points denoting zero effective moment. The dotted curve denotes the extension of a $J = \frac{1}{2}$ Brillouin function above the magnetic transformation indicating a virtual Curie temperature of about 750°K. The (100) reflection has the peak shape normally observed with this spectrometer at all temperatures studied.

HIGH-TEMPERATURE BiMn STRUCTURE

A complete trace of the NOL BiMn sample was obtained at 380°C as shown in Fig. 4(b). The Bi peaks

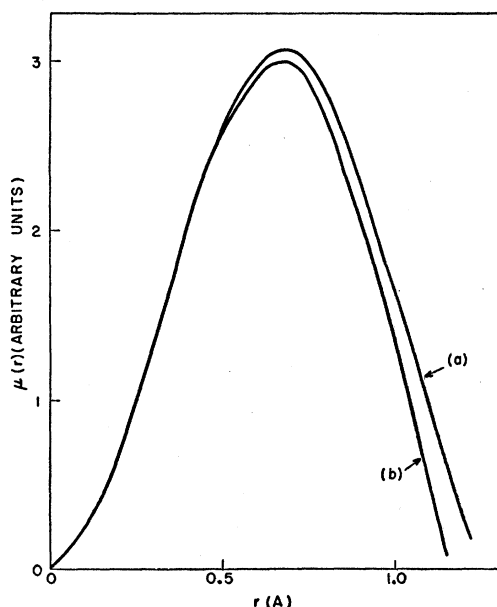


FIG. 6. Qualitative comparison of electron density shift for (a) Mn^{2+} ; (b) BiMn.

are absent since the molten state gives rise to a liquid like scattering not in evidence here. The MnO impurity peaks are present. Table IV lists the observed integrated intensities with the assigned indexes. The lack of resolution at high angles plus temperature broadening requires the summation of many of the adjacent intensities.

In view of the evidence for a paramagnetic state in the temperature range 340–360°C to 445°C, a paramagnetic model was attempted which yielded only nuclear intensities as shown in Table IV under $P_{calc}(para)$. Rough intensity agreement was found when a very large temperature factor was included. As shown in Eq. (1), the temperature factor has been made direc-

TABLE III. BiMn neutron data at 330°C.

hkl	P_{calc}^M	P_{calc}	P_{obs}
001	0	0	Nil ^a
100	248	698	698
101	0	525	525
002	0	193	193
102	43	42	<120
110	33	90	102
003	0	0	Nil
111	0	0	Nil
200	14	121	108
103	0	646	647
201	0		
112	13		
202	6	7	20
004	0	4	Nil
113	0	0	Nil

$a_0=4.31\text{\AA}$, $c_0=6.17\text{\AA}$, $\lambda=1.01_4\text{\AA}$, $C=6.8\text{\AA}^2$, $2B=2.7\text{\AA}^2$, $\mu r=0.4$, $n=2.6\mu_B$; NiAs structure.

^a "Nil" indicates no evidence for a reflection (<10).

tional in an empirical manner since no theoretical calculations for the thermal attenuation of intensities has been made for a uniaxial crystal (hexagonal, tetragonal, etc.). The temperature factor used is similar to that of Hughes¹⁸ and implies in this case a "soft" direction along the c_0 axis with crystal planes perpendicular to the c_0 axis exhibiting large thermal fluctuations or another type of directional loss of lattice perfection. The same temperature factors have been used for each of the three models.

The major discrepancy in the paramagnetic model lies in the low value of the calculated (101) intensity and the (201, 103, 112) intensity group.

In view of Guillaud's predictions of an antiferromagnetic state at high temperature and disregarding the negative susceptibility evidence, an attempt to fit possible antiferromagnetic models was made. Table V gives the possible magnetic reflections with their dependence on spin direction as shown by q^2 . Since no (100) peak was observed, antiferromagnetic models with major moments along the [100] and [110] directions are eliminated. No extra reflections are observed to suggest larger magnetic unit cells. However, a model with moments directed along the c_0 axis remains and

TABLE IV. Observed and calculated BiMn neutron data at 380°C.

hkl	(para)	P_{calc} (anti)	(Disordered) ^a	P_{obs}
001	0	0	0	Nil ^b
100	428	↔ 428	↔ 428	↔ 428
101	482	603(121) ^c	603	603
002	158	158	158	158
102	1	1	2	<11
110	44	44	49	44
111	0	13(13)	0	<10
003	0	0	0	<10
200	80	80	80	75
201, 103, 112	430	438(8)	476	516
202	0.4	0.4	1	Nil
004	2	2	2	Nil
113	0	0.6	0	Nil
210	69	69	68	62
104, 211, 203	159	161(2)	190	198
212	0.4	0.4	1	Nil
300	8	8	9	Nil
301	0	0	0	Nil
114	6	6	7	13
005	0	0	0	Nil
204, 213, 302, 105	115	115	125	135
220	5	5	5	Nil
221	0	0	0	Nil
303	0	0	0	Nil
(115, 310, 214, 311, 222, 205, 006)	110	110	117	95
C (\AA^2)	8.5	8.5	8.5	
$2B$ (\AA^2)	6.3	6.3	6.3	
$n_{eff}(\mu_B)$	0	1.8 ₄	0	
$\lambda=1.01_4\text{\AA}$, $a_0=4.38_5\text{\AA}$, $c_0=6.00_6\text{\AA}$, $\mu r=0.4$.				

^a 0.901 Mn in $000,00\frac{1}{2}$; 0.099 Mn in $\frac{1}{2}\frac{1}{2}\frac{1}{2}, \frac{3}{2}\frac{1}{2}\frac{1}{2}$; Bi in $\frac{1}{2}\frac{1}{2}\frac{1}{2}, \frac{3}{2}\frac{1}{2}\frac{1}{2}$.
^b "Nil" indicates no evidence for a reflection (<10).
^c () denotes magnetic intensity contribution.

¹⁸ E. W. Hughes, J. Am. Chem. Soc. **63**, 1737 (1941).

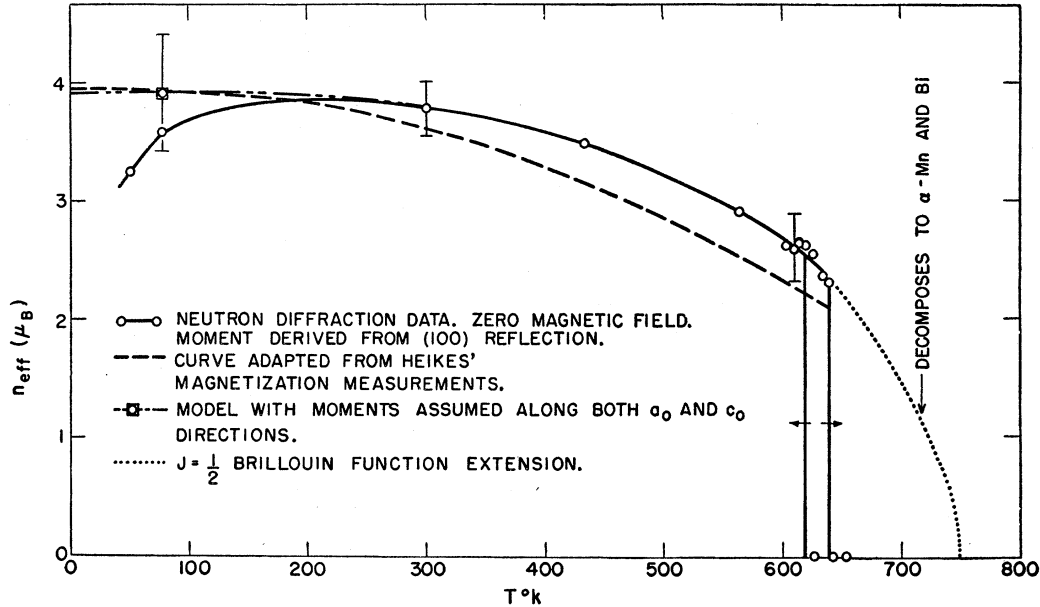


FIG. 7. BiMn magnetization curve by neutron diffraction.

of the first four reflections, only the (101) combination will give a magnetic contribution. This model of an antiferromagnetic structure with moments along the c_0 axis of effective moment of about $1.8\mu_B$ is seen to correct for the low (101) calculated intensity and to give fair agreement with P_{obs} . Some deviation from moment direction along c_0 could be tolerated since the multiplicity of (100) is small and the minimum observable peak is about 10 intensity units.

This antiferromagnetic model is unlikely to be the true state for several reasons. The drop of effective moment from close to $4\mu_B$ to $1.8\mu_B$ at the magnetic transition would suggest an unusual atomic state of Mn. The three measurements of magnetic susceptibility which suggest a paramagnetic state for this temperature range are available even though the temperature range of measurement is small. Guillaud's² susceptibility maximum of 445°C might be explained by the peritectic reaction demonstrated in Fig. 8. At 460°C the BiMn sample has decomposed to α -Mn and molten Bi. Finally, the very large distortion of the unit cell edges would not necessarily be tolerated by such a magnetic transformation without some symmetry or structural change.

TABLE V. Parameters for possible ferromagnetic and antiferromagnetic models.

hkl	F_{mag}^2		q^2			j
	$\uparrow\uparrow$	$\uparrow\downarrow$	[002]	$[100]_{Av}$	$[110]_{Av}$	
001	0	4	0	1	1	2
100	4	0	1	0.500	0.500	6
101	0	4	0.731	0.635	0.635	12
002	4	0	0	1	1	2
c/a			1.429	1.425	1.425	

DISORDERED STRUCTURE

The NiAs unit cell, Fig. 1, has two interstices of symmetry similar to the Bi atom positions. Since one-half the closest interatomic distance in Bi metal¹⁹ is 1.55A and in manganese one-half the separations vary from 1.18A in β -Mn to 1.25 to 1.48A in α -Mn,²⁰ it would appear that occurrence of interstitial Mn atoms would not be unreasonable at high temperature, and this has been proposed in unpublished work by R. R. Heikes. Such a model was attempted and yielded the intensities, P_{calc} (disordered), in Table IV. The number

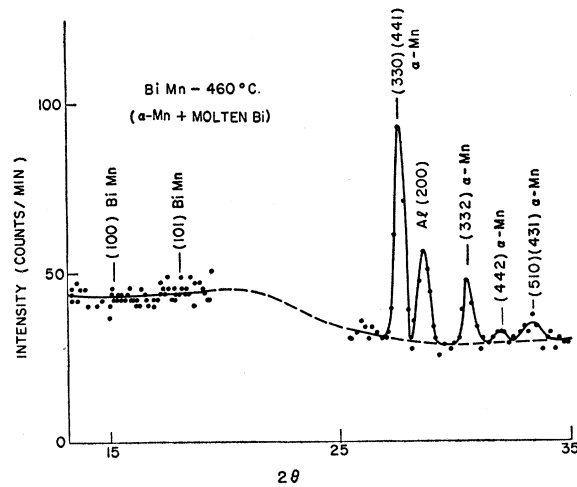


FIG. 8. Neutron diffraction trace of BiMn at 460°C .

¹⁹ L. Pauling and P. Pauling, Acta Cryst. 9, 127 (1956) give the radius of Bi, valence 3, with twelfold coordination as 1.691 A.
²⁰ J. S. Kasper and B. W. Roberts, Phys. Rev. 101, 537 (1956).

of interstitial Mn atoms, denoted Mn^* , was determined by adjusting the usually low (101) reflection to the observed value. This requires 9.9% of the total Mn atoms present to be in the interstitial positions as Mn^* atoms. Crystallographically this is a change from the NiAs-type structure to a disordered $NiIn_2$ -type. It is noted that several additional groups of intensities have better agreement with P_{obs} than is obtained with the previous two models.

The invariance within experimental error of a_0 and c_0 of many samples of BiMn prepared by different procedures, plus the constancy of the magnetic transition temperatures across the phase diagram,¹⁵ supports the assumption made throughout this study that BiMn is stoichiometric.

Very good agreement of the neutron intensities is thus obtained with a disordered $NiIn_2$ model with the assumption of a paramagnetic state for the Mn and Mn^* atoms. Since fair agreement is obtained for an antiferromagnetic model as suggested by Guillaud² and Meyer, one seeks additional data in confirmation.

Consider those atoms which lie on (110) planes in the NiAs-type structure as shown in Fig. 9. Columns of Mn atoms alternate with staggered arrangements of Bi atoms and interstitial sites. In the disordered ($NiIn_2$) structure, the same arrangements of the Bi atoms persist but Mn atoms jump at random into the interstitial sites (Mn^*). Roughly one Mn^* atom is required out of ten starting Mn atoms to obtain neutron intensity agreement. Therefore, each column of Mn atoms over very long distances would be expected on the average to contract. In Fig. 3 an $\sim 3\%$ contraction with rising temperature and an equal expansion upon cooling of c_0 is observed to coincide with the magnetization hysteresis. Thus qualitative agreement of the pronounced distortion of the lattice follows from the disordered model. It is noted that the a_0 axis changes such as to compensate and maintain a continuous volume through the transition. The presence of the

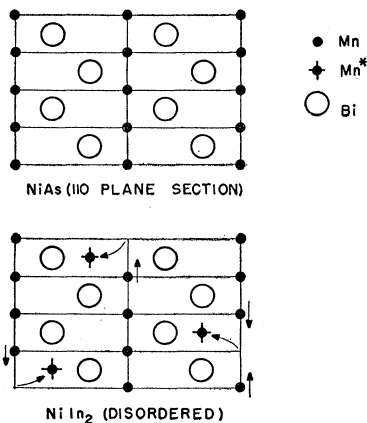


FIG. 9. Atomic arrangement on (110) planes of NiAs and disordered $NiIn_2$ models.

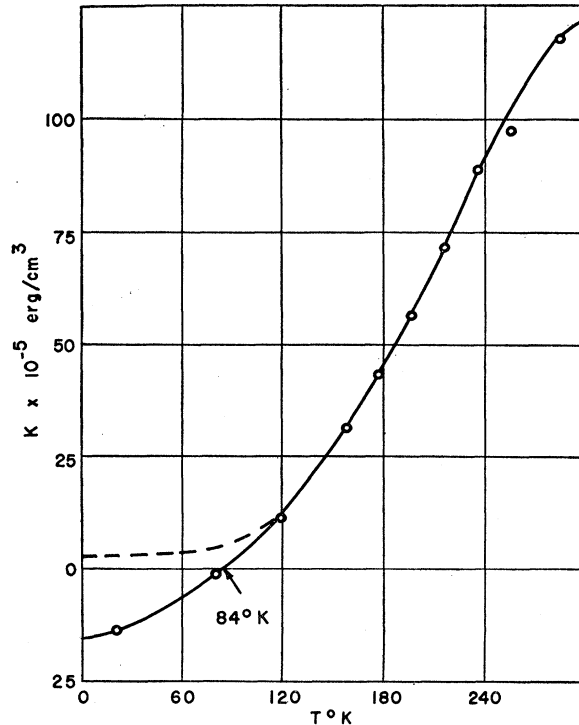


FIG. 10. Magnetocrystalline energy constant, K , as measured by Guillaud.¹ Possible nature of K from neutron diffraction observations made in zero magnetic field.

hysteresis in both the magnetization and cell edge curves is explainable by the disordered model since one may postulate a strain energy to be associated with the motion of the Mn atoms to the interstitial sites. The strain energy would in effect raise the temperature of disordering ($\sim 350^\circ C$) and upon cooling depress the recovery temperature as observed in the $340\text{--}360^\circ C$ hysteresis of the transition. Evidence for a measurable heat of transformation is found at 340° and $360^\circ C$ by Guillaud.¹

Indirect evidence for the disordered model lies in the need for a highly directional temperature factor. The exponential constant $C+2B$ observed for planes lying perpendicular to the c_0 axis is greater than twice the constant $2B$ associated with planes parallel to c_0 . This anisotropy in apparent atomic displacements could well be explained by frozen-in regions of distortion²¹ around a Mn^* atom which would tend to give more attenuation of the coherent reflections of planes perpendicular to the c_0 axis in the same manner as the preferential temperature motion of atoms causes variations in attenuation. Diffuse scattering effects would be different for temperature motion and distortion type attenuation but are not easily measurable with a powder specimen.

The abrupt contraction of the c_0 axis with onset of disorder would appear to coincide with the change from

²¹ K. Huang, Proc. Roy. Soc. (London) A190, 102 (1947).

a ferromagnetic to paramagnetic state. The $d_{\text{Mn-Mn}}$ distance along the c_0 axis abruptly contracts $\sim 3\%$ at the transition between the magnetic states while the distance between a Mn site and an interstitial position denoted as $d_{\text{Mn-Mn}^*}$ in Fig. 3 is essentially continuous. Kasper and Roberts²⁰ have found that spin coupling arrangements in antiferromagnetic α -Mn depend upon both interatomic distance and the necessity of a physically consistent arrangement of spins. Spacings $\geq 2.96\text{\AA}$ in α -Mn were found to be ferromagnetically coupled in agreement with BiMn up to 340–360°C. Above these temperatures $d_{\text{Mn-Mn}}$ is still $> 2.96\text{\AA}$ and the state is found to be paramagnetic. However, the presence of the interstitial Mn* atoms creates regions where no consistent arrangement of spins is possible and therefore no spin alignment would be expected on this basis.

The ferromagnetic properties of BiMn quenched to room temperature from the disordered region, 340–360°C to 445°C, suggest a ferri- or ferromagnetic arrangement of Mn moments or an unusual Mn state as found by Heikes.⁸ Correlation of his quenched cell edge parameters ($c_0 = 5.964\text{\AA}$, $a_0 = 4.339\text{\AA}$) in the form of $d_{\text{Mn-Mn}}$ and $d_{\text{Mn-Mn}^*}$, as shown in Fig. 3, definitely suggests that the disordered phase is being quenched to room temperature and that the Mn* atoms have not had time to relocate on their normal NiAs sites. The extrapolation of $d_{\text{Mn-Mn}}$ from high temperature parallel to that of the equilibrium structure, agrees well with the $d_{\text{Mn-Mn}}$ of the quenched metastable phase.

If a ferrimagnetic model is assumed for the quenched disordered model with an even 10% of Mn* atoms in interstitial positions with moments opposed to the usual magnetization direction, one has a resulting saturation moment of $(0.9-0.1)4\mu_B$ or $3.2\mu_B$ which is considerably above the $1.7\mu_B$ per Mn found by Heikes. Roughly 29% interstitial Mn* atoms would be required to match the observed moment.

TABLE VI. BiMn neutron data: 77.3°K.^a

<i>hkl</i>	$\frac{c_0}{P_{\text{mag}}}$	$\frac{a_0}{P_{\text{mag}}}$	$P_{\text{calc}}^{\text{true}}$	P_{calc}	P_{obs}
001	0	0	0	0	Nil
100	20	20	40	80	80
101	0	0	50	50	50
002	0	8	21	29	29
102	4	14	0.2	18	<32
110	3	3	5	11	12
003	0	0	0	0	<1
111	0	0	0	0	<1
200	2	1	10	13	17
201, 103, 112	1	3	77	81	87
202	1	1	1	3	Nil
004	0	0.2	0.9	1	<3
113	0	0	0	0	Nil
104, 210, 203, 211	1	1	54	56	60
212, 114, 300	6	6	10
005	0	0	Nil
(301, 204, 105, 213, 302)	52	52	47

^a Model: 34% of $3.9\mu_B$ moments along [001], 66% of $3.9\mu_B$ moments along [110]; $a_0 = 4.26\text{\AA}$, $c_0 = 6.06\text{\AA}$, $\lambda = 1.01\text{\AA}$; $\mu_r = 0.4$; no temperature factor used. "Nil" denotes an intensity less than unity.

TABLE VII. Comparison of large particle BiMn intensities at low temperature.

<i>hkl</i>	298°K	P_{obs} 77.3°K	4.2°K	$P_{\text{calc}}^{\text{true}}$ ^a
001	Nil	Nil	Nil	0
100	86	83	72	44.9
101	56	56	56	56.0
002	24	29.5	36	23.8
(201, 112, 113)	88	86	83	85.5

^a Calculated with N₂ data. No temperature correction applied.

When a Mn* atom moves to an interstitial site, five Mn–Mn* pairs are immediately created on the average. If these five nearest neighbors plus the Mn* atom are considered to lose the ferromagnetic exchange necessary for moment alignment due to the unsymmetrical arrangement²⁰ and possibly to the local strains present, roughly 60% of the Mn atoms will not contribute to the saturation moment, leaving $0.4(4\mu_B)$ or $1.6\mu_B$ to be associated on the average with each Mn atom. The moment of this model is of the same order as the $\sim 1.7\mu_B$ observed but requires further study to substantiate.

SPIN ROTATION AT LOW TEMPERATURE

The magnetic measurements of Guillaud show a very rapid decrease in magneto-crystalline energy with decreasing temperature as indicated in Fig. 10. The energy as deduced from magnetization curves, changes sign at 84°K indicating a change in the easy direction of magnetization from along the c_0 axis to somewhere in the basal plane such as the [100] or [110] directions.

A neutron trace taken at 77.3°K and zero magnetic field on the NOL BiMn sample indicates that only part of the moments rotate away from the c_0 axis. The data are listed in Table VI with intensities calculated for the following hypothetical model. Moments are assumed to lie along both the [001] and [110] directions. An intensity balance of the first three observed reflections is then obtained by adjusting the ratio of moments directed along [001] and [110] assuming equal moments for all. When about one-third are directed along [001] and two-thirds lie in the basal plane, the effective moment per Mn is found to be $3.9 \pm 0.5\mu_B$. The magnetic intensities originating from each orientation are shown in Table VI and a point is introduced for n_{eff} in Fig. 7 which extends the magnetization curve to low temperatures with the assumption of this model.

In view of the small mean particle size (28 microns) of the NOL BiMn sample, the possibility of a shape anisotropy effect was suspected. A sample of BiMn was then prepared by alloying small particles of Mn in molten Bi just above the melting point of Bi. The mean particle size of the resulting BiMn was roughly 75μ and was magnetically enriched before study. The BiMn content was finally 55% with adhering Bi the remainder.

In Table VII are listed the observed neutron in-

tensities of the low-angle region which are to be considered qualitative due to the low BiMn content. The reduction of the (100) intensity which signifies that fewer moments are directed along the c_0 axis is noted at 78°K and a further reduction observed when the sample is cooled to liquid He temperature. Conversely the (002) intensity increases as the temperature is lowered in accord with more moments rotating to directions lying in the basal plane. The (101) reflection is used for normalization since only nuclear scattering is possible within the limits of no existing (100) reflection as demonstrated in Table V.

The nature of the ferromagnetic domain structure in BiMn at these low temperatures has not been observed and no obvious differences in the neutron diffraction results are observed between the two samples of different particle size. The incomplete rotation from the c_0 axis of the magnetic moments at 77.3°K in both samples and at 4.2°K in one, however, is clear. The intensity fit noted in Table VI for the NOL BiMn at 77.3°K is interpretable with moments assumed to lie in two specific directions of the lattice although models with all moments directed with the same fixed angle from the c_0 axis would be tenable within experimental limits since magnetic contributions to the (100) and (002) reflections are inversely related by the mode of q^2 variation with moment direction. A loss of hexagonal symmetry would be expected if the moments lay along [101] for instance. It is therefore difficult to specify the exact moment arrangement. If the magnetocrystalline energy is near zero so that continuous linkage of moments is possible throughout the lattice irrespective of the crystal axes, the coherent magnetic intensities would be greatly reduced and additional diffuse scattering due to the arbitrariness of moment directions would occur. Since the coherent intensities at 77.3°K are satisfied with a moment of $3.9\mu_B$ with a spin direction system assumed, the latter model would not appear tenable.

The partial rotation of the magnetic moments as suggested by these measurements would not conflict with a magnetocrystalline energy curve which remained positive at low temperature as tentatively indicated in Fig. 10 by the dashed line. The moments would continue to retain the easy direction of magnetization along c_0 but the low magnetocrystalline energy would permit rotation of spin moment directions of some particles into the basal plane. Closure domains²² could be pictured to give such results, and the suggestion of shape anisotropy has been made by I. S. Jacobs and C. P. Bean of this laboratory to explain the rotation of

²²L. Landau and E. Lifshitz, *Physik. Z. Sowjetunion* 8, 153, (1935).

moment directions based upon the appearance of torque curves made at low temperatures.

CONCLUSIONS

These neutron diffraction measurements on BiMn alloy in the presence of Bi and MnO confirm the magnetization measurements and magnetic structure generally accepted near room temperature. The magnetic moment per Mn atom is found to agree within experimental error with the recent extrapolated value of $3.9\mu_B$ determined by Heikes on high-purity BiMn. The interpretation of the neutron data requires spin-only scattering and a magnetic form factor which is greater at given angle than that found for the Mn^{++} state and qualitatively suggests tighter binding of the $3d$ electrons of the Mn in BiMn.

The extrapolated moment near $4\mu_B$ is consistent with the state Mn^{+++} , which would suggest completion of the outer electron shells of the Bi atom.

A fair match of the neutron intensities observed at 380°C is obtained by assuming an antiferromagnetic arrangement of moments of magnitude $1.8\mu_B$. However, a better fit of intensities is obtained by assuming a disordered structure with no spin alignment of the Mn moments. The disordered structure involves random movement of about 10% of the Mn atoms into large interstitial sites available in the NiAs lattice. This model qualitatively explains the 3% contraction in the c_0 axis coinciding with loss of magnetization and by inferring that strain energy be associated with the displaced Mn atoms would suggest the origin of the magnetization curve hysteresis. The disorder model is in good agreement with the observations and, along with known magnetic susceptibility data, would rule out the antiferromagnetic model.

The arrangement of Mn atoms in the disordered structure suggests an interpretation of the quenched magnetic phase of BiMn reported by Heikes in which 4/10 of the Mn atoms would have aligned spins with the remainder being unaligned.

The magnetic moments do not rotate completely from along c_0 into the basal plane at temperatures below 84°K under zero applied magnetic field. The data suggest the possibility of a positive magnetocrystalline energy at very low temperature.

ACKNOWLEDGMENTS

The author gratefully acknowledges the initial guidance and aid extended by the neutron diffraction groups at Oak Ridge and Brookhaven National Laboratories over a period of several years, and the many exchanges with his colleagues of this laboratory, especially V. C. Wilson, I. S. Jacobs, C. P. Bean, and D. Turnbull.